AUCTORES
Globalize your Research

International Journal of Clinical Case Reports and Reviews
Nan Lu *

Open Access

Review Article

Theoretical investigation on phosphine-catalyzed sequential annulation of 2-arylmethylidene cyanoacetate with Morita–Baylis–Hillman (MBH) carbonate to cyclopentane and diquinane

Nan Lu

College of Chemistry and Material Science, Shandong Agricultural University, Taian 271018, P. R. China.

***Corresponding Author:** Nan Lu, College of Chemistry and Material Science, Shandong Agricultural University, Taian 271018, P. R. China.

Received Date: December 18, 2024 | **Accepted Date:** January 23, 2025 | **Published Date:** February 10, 2025

Citation: Nan Lu, (2025), Theoretical investigation on phosphine-catalyzed sequential annulation of 2-arylmethylidene cyanoacetate with Morita−Baylis−Hillman (MBH) carbonate to cyclopentane and diquinane, *International Journal of Clinical Case Reports and Reviews*, 23(2); **DOI:10.31579/2690-4861/686**

Abstract:

The first theoretical investigation was provided by our DFT calculation on phosphine-catalyzed sequential an-nulation of 2-arylmethylidene cyanoacetate and MBH carbonate. MBH carbonate was initially attacked by PMe3 to generate cation intermediate and carbon dioxide. Then proton abstraction of t-butoxyl anion gives t-butanol and resonance-stabilized zwitterionic intermediate, from which the conjugate addition and subse-quent Michael addition happens with two molecules of 2-arylmethylidene cyanoacetate. Next, the deproto-nation−reprotonation proceeds before SN2' substitution giving desired product cyclopentane. If another molecule of cation intermediate participates in Michael addition followed by isomerization, intramolecular ad-dition, deprotonation−reprotonation and intramolecular SN2 substitution, another product diquinane with two fused five-membered ring is yielded. The deprotonation−reprotonation is rate-limiting for both products. This divergent transformation enables one-pot construction of five or four consecutive stereogenic centers, three or four new C−C bonds and one or two carbocyclic rings via [1 + 2 + 2] or [1 + 2 + 2]/[3 + 2] annulation.

Key words: MBH carbonate; sequential annulation; activated alkene; diquinane; cyclopentane

1.Introduction

As privileged structural subunits, cyclopentanes are ubiquitous in pharmaceuticals and can be found in natural products. In this field, functionalized cyclopentanes and diquinanes have attracted significant interest with selected examples of lycojaponicumin C and calyciphylline N [1,2] due to their effective activity in treating antibacterial, anticancer and rheumatic heart diseases [3,4]. In recent years, a large number of synthetic methods attracted significant attention for construction of these hot topic polysubstituted skeletons in organic synthetic community. For instance, Irie researched total synthesis of putative melognine [5]. Schneider discovered the complex taxane diterpene canataxpropellane [6]. Pan obtained a general strategy for taxane diterpenes [7]. There are also processes such as phosphine-catalyzed asymmetric organic reaction reported by Ni [8], asymmetric reaction catalyzed by chiral tertiary phosphine of Wei and heterocyclic compounds synthesis through nucleophilic phosphine catalysis of Huang [9,10].

A versatile synthon we are interested in is Morita−Baylis−Hillman (MBH) carbonate since it can participate in phosphine-catalyzed annulation bearing allylic alcohol moieties, electron-withdrawing groups and Michael acceptors. Chen reported transformation of MBH adducts from isatins catalyzed by Lewis Bases [11]. Li explored organocatalytic (1 + 4)-annulations of MBH adducts with electron-deficient system [12]. Ma and Shao summarized advances in nucleophilic Lewis Base-catalyzed cycloaddition for synthesis of spirooxindole, reaction of MBH carbonates, scope and mechanism [13,14]. However, the utilization of MBH carbonates is still limited in aspect of phosphine-catalyzed sequential or divergent [4 + 3] and solvent-controlled switchable domino annulation [15-17]. On the other, 2-arylmethylidene cyanoacetates are typical substrates in phosphine-catalyzed annulation as electron-deficient alkenes. Xiao developed remote Friedel−Crafts reaction with α-heteroaryl-substituted cyclic ketones [18]. Liu realized piperidine

derivatives via phosphine-catalyzed (4 + 2) annulation of δ-sulfonamido-substituted enones with 1,1-dicyanoalkenes [19]. Duan utilized allenylic alcohols in tandem annulation [20]. There are also continuous efforts of Wang group in designing phosphine-catalyzed three-component domino reaction.

The progresses in rapid assemble of polysubstituted skeleton are sequential [3 + 2]/[3 + 2] annulation for enantioselective construction of bicyclo[3,3,0]octenes [21], straight-chain ω-amino-α,β-unsaturated carbonyl compounds [22], pyrrolo[3,4-c]quinolines via a $P(NMe_2)_3$-catalyzed [4 + 2] annulation [23] and 2-vinylindolines via α-umpolung/wittig olefination/cyclization cascade process [24]. A breakthrough was controllable three-component domino reaction of activated alkenes with MBH carbonates [25]. Although densely functionalized cyclopentanes and diquinanes were synthesized, how two products were formed in divergent mode during competition between alternative paths? What's the function of phosphine in initial activation of 2-arylmethylidene cyanoacetate? Whether SN2 substitution or deprotonation−reprotonation is rate-limiting for the whole process? How two all-carbon quaternary stereocenters is controlled via [1 + 2 + 2] or [1 + 2 + 2]/[3 + 2] annulation in new carbocyclic rings?

2 Computational details

Structures were optimized at M06-2X/6-31G(d) level with GAUSSIAN09 [26]. Among various DFT methods [27], M06-2X functional has smaller deviation between experimental and calculated value than B3LYP hybrid functional [28,29]. With 6-31G(d) basis set, it can provide best compromise between time consumption and energy accuracy. It was also found to give accurate results for stepwise (2 + 2) cycloaddition, enantioselective (4 + 3) and Diels−Alder reaction [30,31]. Together with good performance on noncovalent interaction, it is suitable for this system [32-34]. To obtain zero-point vibrational energy (ZPVE), harmonic frequency calculations were carried out at M06-2X/6-31G(d) level gaining thermodynamic corrections at 298 K and 1 atm in dichloromethane (DCM). At M06-2X/6-311++G(d,p) level, the solvation-corrected free energies were obtained using integral equation formalism polarizable continuum model (IEFPCM) [35-39] on M06-2X/6-31G(d)-optimized geometries. NBO procedure was performed with Natural bond orbital (NBO3.1) obtaining lone pair and bond to characterize bonding orbital interaction and electronic properties [40-42]. Using Multiwfn_3.7_dev package [43], wave function analysis was explored on Mayer bond order (MBO) and frontier molecular orbital (FMO).

3 Results and Discussion

The mechanism of phosphine-catalyzed sequential annulation of 2-arylmethylidene cyanoacetate **1** with MBH carbonate **2** to cyclopentane **3** and diquinane **4** (Scheme 1). PMe_3 was selected here as model catalyst according to experiment. Illustrated by black arrow of Scheme 2, MBH carbonate **2** was initially attacked by PMe_3 to generate intermediate **A** and carbon dioxide. Then the t-butoxyl anion abstracted a proton to give t-butanol and resonance-stabilized zwitterionic intermediate **B**, from which a conjugate addition to **1** afforded intermediate **C**.

Subsequently, another molecule of **1** was attacked by **C** via Michael addition to deliver intermediate **D**, which was transformed to intermediate **E** via deprotonation−reprotonation process. Through SN2' substitution of intramolecular addition intermediate **F** was obtained, from which the elimination of PMe_3 gave desired product cyclopentane **3** (red arrow). Alternatively, intermediate **G** was produced if another molecule of **A** was attacked by **C**. Next via proton shift, **G** could be isomerized to intermediate **H**, which underwent an intramolecular addition to generate closed five-membered ring of intermediate **I**. Then **I** was transformed to intermediate **J** via deprotonation−reprotonation. An intramolecular SN2 substitution of **J** afforded another five-membered ring of diquinane precursor **K**. After the release of two PMe_3 and one proton, another product diquinane **4** was yielded different from the case of **3** (blue arrow). Figure 1 listed schematic structures of optimized TSs in Scheme 2. Table 1 gave activation energy for all steps.

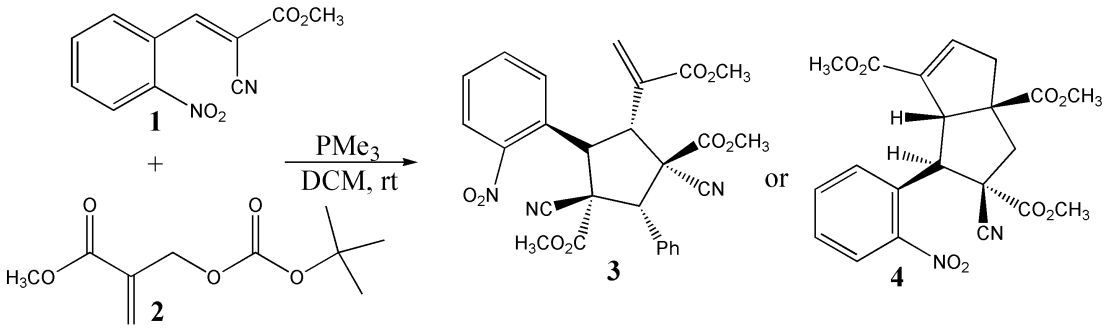

Scheme 1: Phosphine-catalyzed sequential annulation of 2-arylmethylidene cyanoacetate **1** with MBH carbonate **2** to cyclopentane **3** and diquinane **4**.

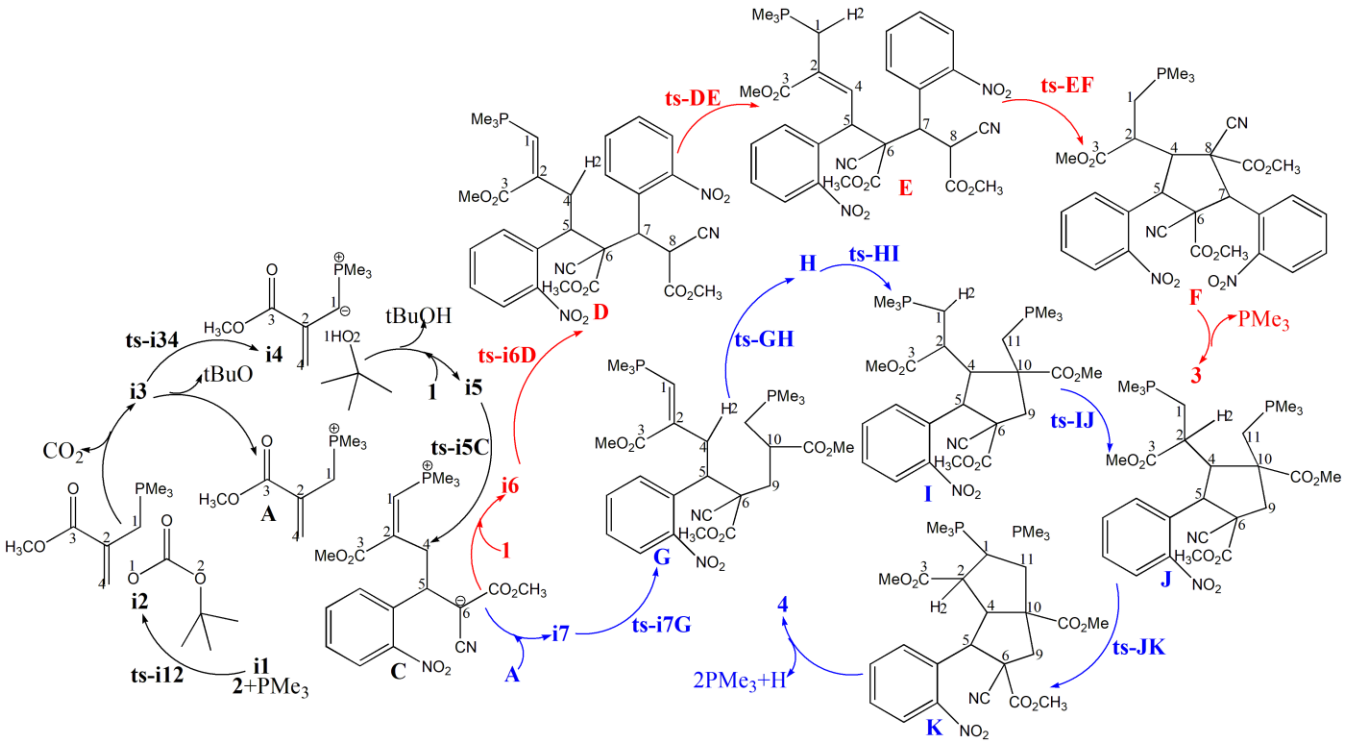

Scheme 2: Reaction mechanism of PMe_3-catalyzed sequential annulation of 2-arylmethylidene cyanoacetate **1** with MBH carbonate **2** to cyclopentane **3** and diquinane **4**.

(a)

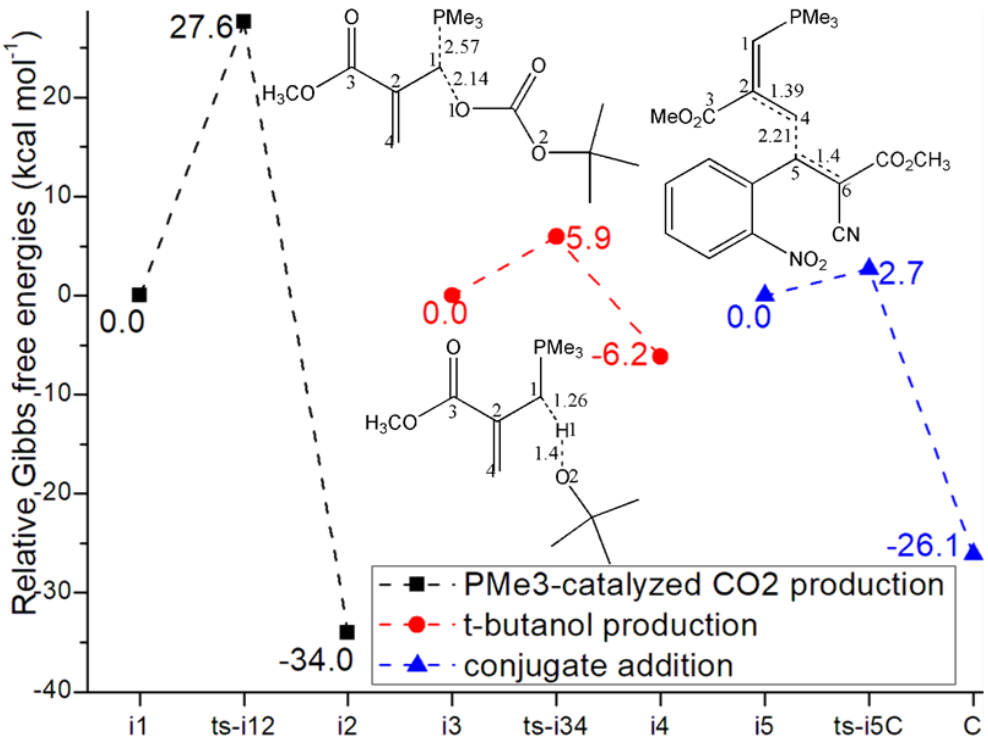

(b)

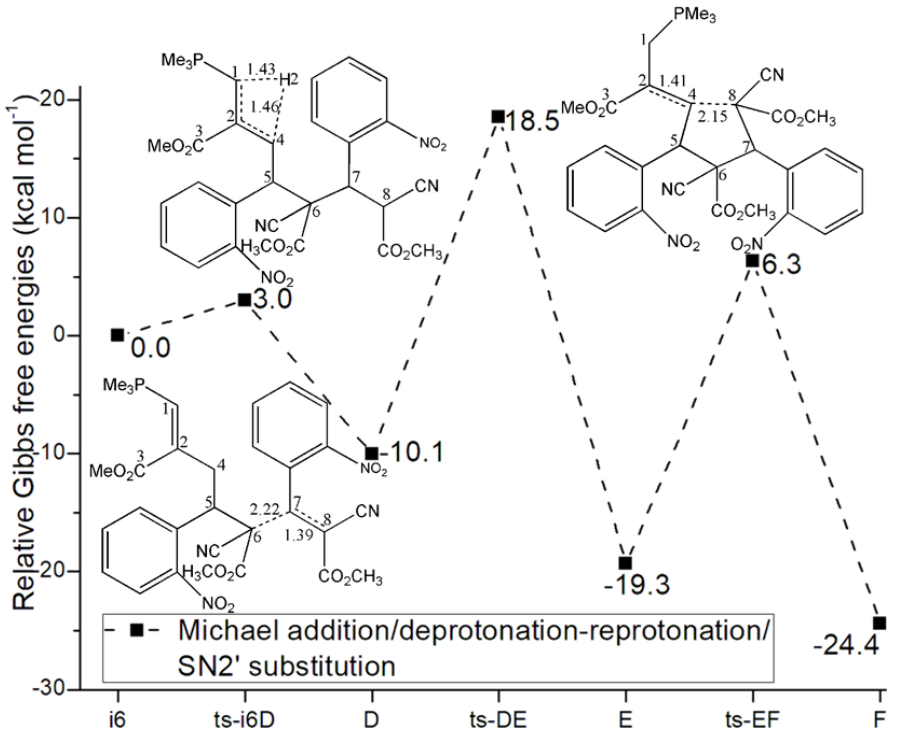

(c)

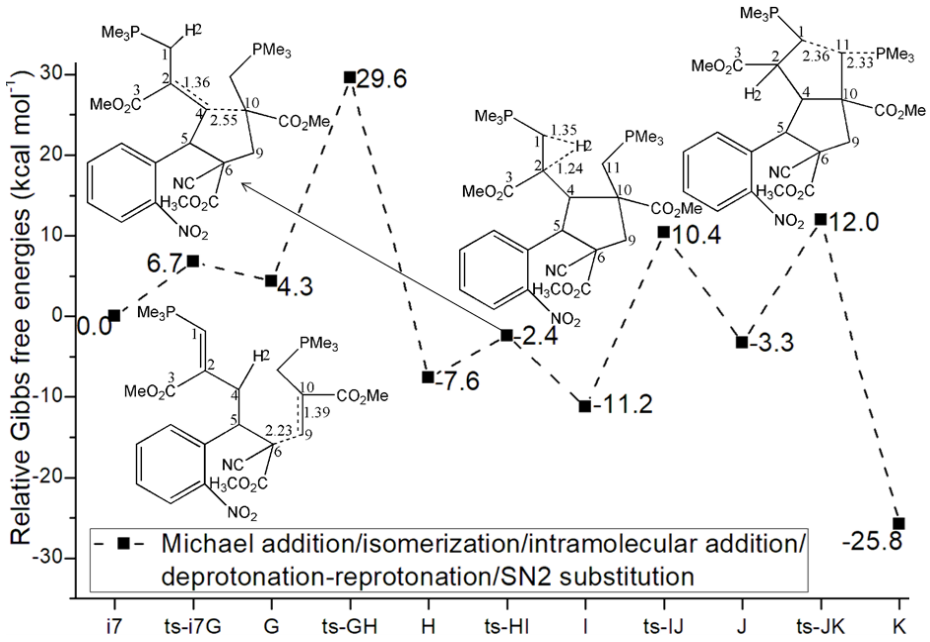

Figure 1: Relative Gibbs free energy profile in solvent phase starting from complex (a) **i1**, **i3**, **i5** (b) **i6** (c) **i7** (Bond lengths of optimized TSs in Å).

TS	$\Delta G^{\neq}_{gas}$	$\Delta G^{\neq}_{sol}$
ts-i12	28.9	27.6
ts-i34	3.0	5.9
ts-i5C	5.8	2.7
ts-i6D	6.2	3.0
ts-DE	29.9	28.6
ts-EF	27.8	25.6
ts-i7G	8.9	6.7

ts-GH	27.4	25.3
ts-HI	7.4	5.2
ts-IJ	25.6	21.6
ts-JK	19.4	15.3

Table 1: The activation energy (in kcal mol^{-1}) of all reactions in gas and solvent

3.1 PMe_3-catalyzed production of carbon dioxide, t-butanol and conjugate addition

Initially, the complex between MBH carbonate **2** and PMe_3 is taken as starting point **i1** (black dash line of Figure 1a), from which the C1-O1 bond is attacked by PMe_3 via **ts-i12** in step 1 with the activation energy of 27.6 kcal mol^{-1} exothermic by -34.0 kcal mol^{-1} producing stable intermediate **A** and carbon dioxide CO_2 binding t-butoxyl anion. The transition vector includes cleavage of C1···O1 and linkage of C1···P (2.14, 2.57 Å) (Figure S1a). Typical C1-P single bond is generated in **A** with positive charge focused on P atom.

After the leaving of CO_2, **A** and t-butoxyl anion assembles **i3** (red dash line of Figure 1a), which initiates proton transfer via **ts-i34** in step 2 with low activation energy of 5.9 kcal mol^{-1} exothermic by -6.2 kcal mol^{-1} generating **i4**. Though this process, a proton of **A** on C1 is abstracted by t-butoxyl anion O2 giving t-butanol and resonance-stabilized zwitterionic intermediate **B**. The transition vector also suggests proton H1 transfer from C1 to O2 (1.26, 1.4 Å) (Figure S1b). Compared with cation **A**, **B** is neutral with positively charged P and negative C1 or C4 in resonant mode.

After the removal of t-butanol, the addition of **1** to **B** forms **i5** taken as new starting point of the following step 3 (blue dash line of Figure 1a). That is conjugate addition taking place via **ts-i5C** with activation energy of 2.7 kcal mol^{-1} affording stable intermediate **C** exothermic by -26.1 kcal mol^{-1}. The transition vector is about nucleophilic attack of negative C4 to C5 and resulting elongation of C2=C4, C5=C6 double bond to single (2.21, 1.39, 1.4 Å) (Figure S1c). As the formation of C4-C5 single bond in **C**, the negative charge is shifted on C6 ready to initiate next step.

3.2 Michael addition/deprotonation−reprotonation/SN2' substitution

Subsequently, another molecule of **1** was added with positive C7 of C7=C8 double bond as counterparts of previous C5=C6. Binding **C** and **1**, **i6** is taken as the starting point for next three steps (black dash line of Figure 1b). Michael addition readily occurs via **ts-i6D** in step 4 with activation energy of 3.0 kcal mol^{-1} exothermic by -10.1 kcal mol^{-1} delivering intermediate **D**. The transition vector corresponds to the approaching of carbanion C6 to alkene positive C7 along with the stretching of C7=C8 from double to single (2.22, 1.39 Å) (Figure S1d). C6-C7 single bond is available in **D**.

D was transformed to intermediate **E** via deprotonation−reprotonation process. A further proton shift happens via **ts-DE** in step 5 with increased activation energy of 28.6 kcal mol^{-1} exothermic by -19.3 kcal mol^{-1}. The transition vector reveals detailed atomic motion about proton H2 transfer from sp3 hybrid C4 to sp2 C1 (1.46, 1.43 Å). The change of hybrid makes the movement of double bond from C1=C2 to C2=C4 as well as negative charge shifting to C4 preparing for subsequent SN2' substitution.

An intramolecular addition of carbanion C4 to C8 proceeds via **ts-EF** in step 6 with activation energy of 25.6 kcal mol^{-1} exothermic by -24.4 kcal mol^{-1}realizing crucial ring closure. This process is illustrated as SN2' substitution according to the transition vector composed of C4···C8 approaching and concerted C2=C4 double bond stretching to single (2.15, 1.41 Å). Once C4-C8 single bond is completed, the five-membered carbocycle intermediate **F** is obtained, from which the elimination of PMe_3 yields desired product cyclopentane **3**.

3.3 Michael addition/isomerization/intramolecular addition/deprotonation−reprotonation/SN2 substitution

Alternatively if another molecule of **A** is attacked by **C**, **i7** is located as starting point of next four steps (black dash line of Figure 1c). Although the step 4 is also Michael addition easy to occur via **ts-i7G** with activation energy of 6.7 kcal mol^{-1}, it is required to endothermic by 4.3 kcal mol^{-1} delivering intermediate **G**. The transition vector corresponds to the approaching of carbanion C6 to terminal alkene positive C9 and elongation of C9=C10 double bond (2.23, 1.39 Å) (Figure S1e).

Next via proton shift of **ts-GH**, **G** could be isomerized to intermediate **H** in step 5 with activation energy of 25.3 kcal mol^{-1} exothermic by -7.6 kcal mol^{-1}. The transition vector reveals proton transfer mode of C4···H2···C1 (Figure S1f) just like the case of **ts-DE**. Similar with **E**, **H** also involves sp3 hybrid C1 and nucleophilic C4 undergoing intramolecular addition leading to the first five-membered ring of intermediate **I** with C4-C10 single bond. This step 6 is via **ts-HI** with activation energy of 5.2 kcal mol^{-1} affording **I** exothermic by -11.2 kcal mol^{-1}.

Then **I** was transformed to intermediate **J** via deprotonation−reprotonation of **ts-IJ** in step 7 with the activation energy of 21.6 kcal mol^{-1} exothermic by -3.3 kcal mol^{-1}. The transition vector corresponds to C1 donating proton H2 to C2 making the enhanced nucleophilic ability of itself (1.35, 1.24 Å) (Figure S1g). Thus from **J**, the final intramolecular SN2 substitution occurs via **ts-JK** in step 8 with a barrier of 15.3 kcal mol^{-1} exothermic by -25.8 kcal mol^{-1} giving the second five-membered ring of diquinane precursor **K**. Demonstrated by the transition vector, this process is typical SN2 substitution with swing of sp2 hybrid C11 between C1 and P (2.36, 2.33 Å) (Figure S1h). The simultaneous bonding of C1···C11 and breaking of C11···P are accomplished in **K**, from which another product diquinane **4** is produced after the release of two PMe_3 and elimination of one proton H2 on C2. **4** contains C1=C2 double bond and two fused five-membered ring. Comparatively, the deprotonation−reprotonation in step 5 is determined to be rate-limiting consistent for both two products **3** and **4** in phosphine-catalyzed sequential annulation.

4 Conclusions

The first theoretical investigation was provided by our DFT calculation on phosphine-catalyzed sequential annulation of 2-arylmethylidene cyanoacetate and MBH carbonate. MBH carbonate was initially attacked by PMe_3 to generate cation intermediate and carbon dioxide. Then proton abstraction of t-butoxyl anion gives t-butanol and resonance-stabilized zwitterionic intermediate, from which the conjugate addition and

subsequent Michael addition happens with two molecules of 2-arylmethylidene cyanoacetate. Next, the deprotonation−reprotonation proceeds before SN2' substitution giving desired cyclopentane product along with recovered PMe_3. Alternatively, if another molecule of cation intermediate participates in Michael addition followed by isomerization, intramolecular addition, deprotonation−reprotonation and intramolecular SN2 substitution, another product diquinane with two fused five-membered ring is yielded after the release of two PMe_3 and one proton. The deprotonation−reprotonation in step 5 is determined to be rate-limiting for both two products in phosphine-catalyzed sequential annulation. This divergent transformation enables one-pot construction of five or four consecutive stereogenic centers, three or four new C−C bonds and one or two carbocyclic rings via [1 + 2 + 2] or [1 + 2 + 2]/[3 + 2] annulation.

Electronic Supplementary Material

Supplementary data available: [Computation information and cartesian coordinates of stationary points; Calculated relative energies for the ZPE-corrected Gibbs free energies (ΔG_{gas}), and Gibbs free energies (ΔG_{sol}) for all species in solution phase at 298 K.]

Author contributions: Conceptualization, Nan Lu; Methodology, Nan Lu; Software, Nan Lu; Validation, Nan Lu; Formal Analysis, Nan Lu; Investigation, Nan Lu; Resources, Nan Lu; Data Curation, Nan Lu; Writing-Original Draft Preparation, Nan Lu; Writing-Review & Editing, Nan Lu; Visualization, Nan Lu; Supervision, Nan Lu; Project Administration, Nan Lu; Funding Acquisition, Nan Lu. All authors have read and agreed to the published version of the manuscript.

Funding: This work was supported by Key Laboratory of Agricultural Film Application of Ministry of Agriculture and Rural Affairs, P.R. China.

Conflict of interest: The authors declare no conflict of interest.

References

1. Wang, X.-J.; Zhang, G.-J.; Zhuang, P.-Y.; Zhang, Y.; Yu, S.-S. et al. (2012). Lycojaponicumins A−C, Three Alkaloids with an Unprecedented Skeleton from Lycopodium japonicum. Org. Lett.14, 2614−2617.
2. Yahata, H.; Kubota, T.; Kobayashi, J. (2009). Calyciphyllines N−P, Alkaloids from Daphniphyllum calycinum. *J. Nat. Prod*. 72, 148−151.
3. Jiang, J.-H.; Zhang, W.-D.; Chen, Y.-G. (2016). Phytochemical and Pharmacological Properties of the Genus Melodinus−A Review. *Trop. J. Pharm*. Res. 14, 2325−2344.
4. Teng, S.-F.; Li, F.- R.; Cui, Q.-M.; Khan, A.; He, T. et al. (2023). A Review on the Genus Melodinus: Traditional Uses, Phytochemical Diversity and Pharmacological Activities of Indole Alkaloids. Phytochemistry Rev. DOI: 10.1007/s11101-023-09871-2.
5. Irie, Y.; Yokoshima, S. (2024). Total Synthesis of Putative Melognine. J. Am. Chem. Soc. 2024, 146, 9526−9531.
6. Schneider, F.; Samarin, K.; Zanella, S.; Gaich, T. (2020). Total Synthesis of the Complex Taxane Diterpene Canataxpropellane. Science, 367, 676−681.
7. Pan, L.; Schneider, F.; Ottenbruch, M.; Wiechert, R.; List, T. et al. (2024). A General Strategy for the Synthesis of Taxane Diterpenes. Nature, 632, 543-549.
8. Ni, H.; Chan, W.-L.; Lu, Y. (2018). Phosphine-Catalyzed Asymmetric Organic Reactions. Chem. Rev. 118, 9344−9411.
9. Wei, Y.; Shi, M. (2020). Asymmetric Reactions Catalyzed by Chiral Tertiary Phosphines. Chin. J. Chem, 38, 1395−1421.
10. Huang, Y.; Liao, J.; Wang, W.; Liu, H.; Guo, H. (2020). Synthesis of Heterocyclic Compounds through Nucleophilic Phosphine Catalysis. Chem. Commun. 56, 15235−15281.
11. Chen, Z.-C.; Chen, Z.; Du, W.; Chen, Y.-C. (2020). Transformations of Modified Morita-Baylis-Hillman Aducts from Isatins Catalyzed by Lewis Bases. Chem. Rec. 20, 541−555.
12. Chen, X.; Li, P. (2023). Organocatalytic (1 + 4)-Annulations of MBH Adducts with Electron-Deficient Systems. Chem. Rec. 23, No. e202300152.
13. Li, Q.-F.; Ma, J.; Meng, J.; Li, E.-Q. (2023). Recent Advances in Nucleophilic Lewis Base-Catalyzed Cycloadditions for Synthesis of Spirooxindoles. Adv. Synth. Catal. 365, 4412−4439.
14. Shao, Y.; Zhang, L.; Meng, X. (2024). Recent Advances in Reactions of MBH Carbonates, Scope and Mechanism. Asian. J. Org. Chem. DOI: 10.1002/ajoc.202400237.
15. Chen, J.; Huang, Y. (2017). Phosphine-Catalyzed Sequential [4 + 3] Domino Annulation/Allylic Alkylation Reaction of MBH Carbonates: Efficient Construction of Seven-Membered Heterocycles. Org. Lett. 19, 5609−5612.
16. Jia, J.; Yu, A.; Ma, S.; Zhang, Y.; Li, K. et al. (2017). Solvent-Controlled Switchable Domino Reactions of MBH Carbonate: Synthesis of Benzothiophene Fused α-Pyran, 2,3-Dihydrooxepine, and Oxatricyclodecene Derivatives. Org. Lett. 19, 6084−6087.
17. Chen, J.; Yin, Z.; Huang, Y. (2019). Phosphine-Catalyzed Divergent [4 + 3] Domino Annulations of CF 3 -Containing Imines with MBH Carbonates: Construction of Perfluoroalkylated Benzazepines. Org. Lett. 21, 7060−7064.
18. Xiao, B.-X.; Shi, C.-H.; Liang, S.-Y.; Jiang, B.; Du, W. et al. (2019). Remote Friedel−Crafts Reaction with α-Heteroaryl-Substituted Cyclic Ketones via HOMO Activation of Lewis Bases. Org. Lett. 21, 7554−7557.
19. Liu, M.; Zhou, L.; Shi, W.; Hu, Y.; Liao, J. et al. (2021). Phosphine-Catalyzed (4 + 2) Annulation of δ-Sulfonamido-Substituted Enones with 1,1-Dicyanoalkenes: Synthesis of Piperidine Derivatives. Org. Lett. 23, 7703−7707.
20. Duan, Z.; Liu, M.; Zheng, B.; Tang, Y.; Du, J. (2023). Phosphine-Catalyzed Tandem Annulation of Allenylic Alcohols with 1,1-Dicyanoalkenes. Org. Lett. 25, 3298−3302.
21. Wang, N.; Lang, Y.; Wang, J.; Wu, Z.; Lu, Y. (2022). Phosphine-Catalyzed Sequential [3 + 2]/[3 + 2] Annulation between Allenoates and Arylidenemalononitriles for the Enantioselective Construction of Bicyclo[3,3,0]octenes and Cyclopenta[c]quinolinones. Org. Lett. 24, 3712−3716.
22. Li, S.; Li, X.; Yao, H.; Tan, M.; Xu, D. (2024). Straight-Chain ω-Amino-α,β-Unsaturated Carbonyl Compounds: Versatile Synthons for the Synthesis of Nitrogen-Containing Heterocycles via Organocatalytic Reactions. Org. Chem. Front. 11, 236−253.
23. Chen, Z.; Xiong, D.; Wang, N.; Zhang, Y.; Yao, H. et al. (2024). Concise Synthesis of Pyrrolo[3,4-c]quinolines via a P(NMe2)3-Catalyzed [4 + 2] Annulation followed by a Zn/AcOH-Mediated Reduction−Hydro-amination−Isomerization. Org. Chem. Front. 11, 2762−2767.
24. Li, S.; Xu, D.; Yao, H.; Tan, M.; Li, X. et al. (2024). Facile Synthesis of 2-Vinylindolines via a Phosphine-Mediated α-Umpolung/Wittig Olefination/Cyclization Cascade Process. Chem. Commun. 2024, 60, 6773−6776.
25. Li, Y.; Hu, X.; Li, B.; Zhang, S.; Yao, H. et al. (2024). Controllable Phosphine-Catalyzed Three-Component Domino Reaction of Activated Alkenes with Morita−Baylis−Hillman (MBH) Carbonates: Divergent Synthesis of Densely Functionalized Cyclopentanes and Diquinanes. Org. Lett.

https://doi.org/10.1021/acs.orglett.4c03089
26. Frisch, M. J.; Trucks, G. W.; Schlegel, H. B. et al. (2010). Gaussian 09 (Revision B.01), Gaussian, Inc., Wallingford, CT.
27. Stephens, P. J.; Devlin, F. J.; Chabalowski, C. F.; Frisch, M. (1994). J. Ab initio Calculation of Vibrational Absorption and Circular Dichroism Spectra Using Density Functional Force Fields, J. Phys. Chem. 98, 11623-11627.
28. Becke, A. D. (1996). Density-functional thermochemistry. IV. A new dynamical correlation functional and implications for exact-exchange mixing. J. Chem. Phys. 104, 1040-1046.
29. Lee, C. T.; Yang,W. T.; Parr, R. G. (1988). Development of the Colle-Salvetti correlation-energy formula into a functional of the electron density. Phys. Rev. B, 37, 785-789.
30. Li, X.; Kong, X.; Yang, S.; Meng, M.; Zhan, X. (2019). Bifunctional Thiourea-Catalyzed Asymmetric Inverse-Electron-Demand Diels-Alder Reaction of Allyl Ketones and Vinyl 1,2-Diketones via Dienolate Intermediate, Org. Lett. 21, 1979-1983.
31. Krenske, E. H.; Houk, K. N.; Harmata, M. (2015). Computational Analysis of the Stereochemical Outcome in the Imidazolidinone-Catalyzed Enantioselective (4 + 3)-Cycloaddition Reaction, J. Org. Chem. 80, 744-750.
32. Lv, H.; Han, F.; Wang, N.; Lu, N.; Song, Z. et al. (2022). Ionic Liquid Catalyzed C-C Bond Formation for the Synthesis of Polysubstituted Olefins. Eur. J. Org. Chem, e202201222.
33. Zhuang, H.; Lu, N.; Ji, N.; Han, F.; Miao, C. (2021). Bu4NHSO4-Catalyzed Direct N-Allylation of Pyrazole and its Derivatives with Allylic Alcohols in Water: A Metal-free, Recyclable and Sustainable System. Advanced Synthesis & Catalysis, 363, 5461-5472.
34. Lu, N.; Liang, H.; Qian, P.; Lan, X.; Miao, C. (2020). Theoretical investigation on the mechanism and enantioselectivity of organocatalytic asymmetric Povarov reactions of anilines and aldehydes. Int. J. Quantum Chem. 120, e26574.
35. Tapia, O. (1992). Solvent effect theories: Quantum and classical formalisms and their applications in chemistry and biochemistry. J. Math. Chem. 10, 139-181.
36. Tomasi, J.; Persico, M. (1994). Molecular Interactions in Solution: An Overview of Methods Based on Continuous Distributions of the Solvent. Chem. Rev. 94, 2027-2094.
37. Simkin, B. Y.; Sheikhet, I. (1995). Quantum Chemical and Statistical Theory of Solutions—A Computational Approach, Ellis Horwood, London.
38. Tomasi, J.; Mennucci, B.; Cammi, R. (2005). Quantum Mechanical Continuum Solvation Models. Chem. Rev. 105, 2999-3093.
39. Marenich, A. V.; Cramer, C. J.; Truhlar, D. G. (2009). Universal Solvation Model Based on Solute Electron Density and on a Continuum Model of the Solvent Defined by the Bulk Dielectric Constant and Atomic Surface Tensions. J. Phys. Chem. B, 113, 6378–6396.
40. Reed, A. E.; Weinstock, R. B.; Weinhold, F. (1985). Natural population analysis. J. Chem. Phys. 83, 735-746.
41. Reed, A. E.; Curtiss, L. A.; Weinhold, F. (1988). Intermolecular interactions from a natural bond orbital donor-acceptor view point. Chem. Rev. 88, 899-926.
42. Foresman, J. B.; Frisch, A. (1996). Exploring Chemistry with Electronic Structure Methods, 2nd ed., Gaussian, Inc., Pittsburgh.
43. Lu, T.; Chen, F. (2012). Multiwfn: A multifunctional wavefunction analyzer. J. Comput. Chem. 33, 580-592.

DOI:10.31579/2690-4861/686